Desalination and Water Treatment
www.deswater.com

doi: 10.5004/dwt.2022.28668

267 (2022) 240–252
August

Development of biomass activated carbon using full factorial design for the removal of methyl orange from aqueous solution

B. Bouider, K. Rida*

Laboratoire d'Interactions Matériaux et Environnement (LIME), Université Mohamed Seddik Ben Yahia –Jijel, Algeria, emails: rida_kamel2001@yahoo.fr (K. Rida), bouiderbadis@gmail.com (B. Bouider)

Received 7 February 2022; Accepted 2 July 2022

ABSTRACT

In this work, different factors which interfere in the preparation of activated carbon from *Brachychiton populneus* by chemical activation were studied in order to determine the optimal conditions used in full factorial 2^3 experimental design. The factors and levels included are activation temperature (600°C and 800°C), activation time (60 and 90 min) and type of activating agent (NaOH and $FeCl_3$). The yield of activated carbon, total volume of the pores of activated carbon and the methyl orange adsorption were chosen as a measure of the optimization. The samples were characterized by Brunauer–Emmett–Teller surface area, scanning electron microscopy, Fourier transform infrared spectroscopy and pH_{pzc}, surface functions based on Boehm method. The results reveal that the most influential factors on the yield and the methyl orange adsorption are activation temperature, activation time and type of activating agent and the presence of a significant interaction between activation temperature and activation time in both cases. The optimum conditions to prepare activated carbons were obtained using 800°C activation temperature, 90 min activation time, and NaOH activating agent while the maximal specific surface area was found to be 803 $m^2 \cdot g^{-1}$ and the removal of methyl orange was found to be 95%. This work showed that *Brachychiton populneus* shells are a good precursor for the production of activated carbon, by chemical activation, with high performance to be used in water treatment applications.

Keywords: Factorial design; Activated carbon; *Brachychiton populneus*; Adsorption; Anionic dye

1. Introduction

Due to its comparatively high adsorption performance and applicability, activated carbon (AC) is a porous material with a wide range of uses in water treatment and purification [1,2]. Commercially, ACs have been widely obtained from non-renewable sources such as coal, lignite, and peat. The main limitation regarding the application of AC is the high cost. The characteristics of activated carbon mainly depend on both the nature of the precursor and the preparative conditions nature of the precursor [3]. One of the main challenges in the commercial manufacture of ACs is to identify new cheap precursors.

Previously, the activated carbon was produced with a variety of raw materials from biomass wastes. Also, the abundance and availability of biomasses assure us using them as a precursor for the production of activated carbon of low-cost [4]. As a result, a variety of lignocellulosic biomasses have been used as raw materials for manufacturing-activated carbon, including apricot stones [5], olive stones [6], date pits [7], and sawdust [8]. The reason for this is that these raw materials are renewable and potentially less expensive to manufacture.

Several activated carbons (ACs) with high surface area and developed porosity from diverse lignocellulosic materials have been reported in the literature [9–12]. The

* Corresponding author.

adsorption capacity of AC is primarily determined by three factors: high surface area, microporous character, and chemical nature of their surface, all of which are influenced by the AC fabrication procedure [13]. Physical or chemical activation can be used to create activated carbon compounds. Chemical activation, on the other hand, provides several advantages. Different activation agents, such as $ZnCl_2$, H_3PO_4, and NaOH, have been examined in the literature in the past [14,15]. In recent years, $FeCl_3$ activation has gotten a lot of attention. It is low-cost and environmentally friendly, and it produces magnetic activated carbons [16]. When compared to commercial ACs, biomass waste-derived ACs exhibit greater adsorption performance due to careful selection of biomass waste, preparation procedures, and careful control of preparation and adsorption conditions [17,18].

Many aspects influence the preparation of a high-quality AC. In earlier investigations, impregnation ratio (IR), activation temperature, and activation duration were determined to be the most relevant parameters [19,20]. Optimizing the preparation conditions necessitates the use of an appropriate experimental design. The factorial experimental design, which involves altering all of the variables from one trial to the next, has been shown to be a powerful tool for studying the influence of variables as well as the interactions of two or more variables with fewer experiments [21,22].

In this work, two objectives have been targeted. The first is to use the *Brachychiton populneus* shell as a raw material for the production of activated carbon; it is a promising candidate among the agricultural wastes because it is quite abundant in the Mediterranean countries and can be activated either physically or chemically. To our knowledge, there are no published reports on these cores for the preparation for activated carbon. The second is carried out using a 2^3 factorial design in order to examine the main effects and the interactions between activation temperature, activation time and the type of activating reagent (NaOH or $FeCl_3$). Methyl orange (MO) was chosen in this study as a model compound for removing organic contaminants and colored bodies from aqueous solutions. The performances of the prepared activated carbons (expressed in terms of iodine number and specific surface area) are studied.

2. Materials and methods

2.1. Materials

The biomass used in this study is the Fruit crust of ripe *Brachychiton populneus*, as indicated in Fig. 1, obtained from the region of Jijel (East of Algeria). The samples were washed with distilled water and dried in libber air ambient temperature for several days, then crushed and selected for the preparation. All Chemicals and reagents used in the study were of analytical grade supplied from Sigma–Aldrich (Germany).

2.2. Preparation of activated carbons

The activated carbons were prepared from waste biomass in two phases. The biomass was first carbonized for 2 h at 300°C. The second experiment involved chemical activation of carbonized materials using two agents ($FeCl_3$ and NaOH) at the same rate of impregnation (1: 2) at 60°C–80°C for 4 h. After washing with distilled water and drying in an oven at 105°C, out a heat treatment of the material in a tube furnace at 600°C and 800°C for 1 h and 1 h 30 min. After obtaining the activated materials, the samples were rinsed with deionized water until the pH of the solution approached neutrality, and then dried in an oven at 105°C. The yield of the activated carbon was estimated with the following equation:

$$\text{Yield}(\%) = \frac{W_{ac}}{W_i} \times 100 \quad (1)$$

where w_i is the initial mass of biomass (g) and w_{ac} the mass of the resulting activated carbon (g).

2.3. Characterization

The surface area and pore volumes of the activated carbons were obtained on a surface area analyzer (Micromeritics ASAP 2020) through N_2 adsorption/desorption at 77 K. Initially samples were out gassed at 150°C for 7 h and the resulting surface areas (S_{BET}) were measured using BET (Brunauer–Emmett–Teller equation) method. The surface area of micropores (S_{micro}), external surface area (S_{ext}) and volume of micropores (V_{micro}) were obtained using the *t*-plot method. The surface morphologies of the activated carbons were also evaluated by a scanning electron microscope (SEM) using a PHILIPS XL-30 ESEM apparatus. The Fourier transform infrared (FTIR) spectra of the activated carbons prepared as KBr pellets were recorded in the transmission mode between 4,000 and 400 cm^{-1} using an FTIR spectroscope (FTIR-8400 Shimadzu). The chemical property analyses were done by measuring the point of zero charge or pH_{pzc} determined using the pH drift method [8]. While for quantifying total acidity and the total basicity, titration method was carried out based on Boehm method [23].

Fig. 1. The *Brachychiton populneus* biomass.

2.4. Adsorption experiments

Batch adsorption experiments were performed in flasks containing a defined amount of adsorbent (1 g·L^{-1}) and 20 mg·L^{-1} of desired concentration of MO solution. These flasks were kept in a shaker of 250 rpm at 25°C. After adsorption, the residual concentration of MO was determined by spectrophotometric method at 462 nm. The suspensions were stirred for 2 h, thereafter there was no significant change in the concentration of MO at equilibrium. The percentage removal of the methyl orange (MO) at equilibrium was calculated using the following equation:

$$\text{Removal dye}(\%) = \frac{C_0 - C_e}{C_0} \times 100 \quad (2)$$

where C_0 is the initial dye concentration and C_e (mg·L^{-1}) is the concentrations of dye at equilibrium.

2.5. Full factorial 2^3 design

A full factorial 2^3 design with three operational factors each in two levels was used to optimize the preparation conditions of the *Brachychiton populneus*-based ACs and the MO removal efficiency. The activation agent (x_1), activation temperature (x_2), and activation time (x_3) are the three explored parameters in this study. Table 1 shows the high and low levels for each of the 2^3 factorial designs. According to some preliminary experiments, the low and high amounts for the components were chosen. Table 2 shows the design matrix of uncoded values for the components, as well as the response in terms of yield (Y_1), total volume of the pores of activated carbon (Y_2), and percent elimination of MO (Y_3) for all experimental runs, including repeats.

Table 1
Levels of independent process variables used in full factorial design

Independent variable	Symbol	Coded level	
		Low level (−1)	High level (+1)
Activating agent	x_1	NaOH	$FeCl_3$
Temperature (°C)	x_2	600	800
Activation time (min)	x_3	60	90

Table 2
The design matrix for the factors and the response

N	Experimental plan			Measured responses		
	x_1	x_2	x_3	Yield Y_1	Total volume of the pores Y_2	Removal of MO (%) Y_3
1	NaOH	600	60	48.00	0.191	38.350
2	$FeCl_3$	600	60	44.22	0.221	28.130
3	NaOH	800	60	56.50	0.298	78.520
4	$FeCl_3$	800	60	67.00	0.291	62.270
5	NaOH	600	90	51.25	0.368	41.620
6	$FeCl_3$	600	90	57.98	0.228	34.840
7	NaOH	800	90	68.60	0.503	95.110
8	$FeCl_3$	800	90	70.10	0.335	95.250

$$Y = a_0 + b_1x_1 + b_2x_2 + b_3x_3 + b_{12}x_1x_2 + b_{13}x_1x_3 + b_{23}x_2x_3 + b_{123}x_{123} \quad (3)$$

where, respectively, Y denotes the theoretical response function, a_0 denotes the global mean, and b_i and b_{ij} denote the regression coefficients for main factor effects and interactions. To examine the effects as well as the statistical parameters, the findings of the experimental design were evaluated using Minitab 16 statistical software.

2.6. Desorption and reusability of the adsorbent

To evaluate the reusability of the optimum activated carbon (CAB4) after MO adsorption, five regeneration cycles were performed. Adsorption tests were performed with 50 mL of MO dye aqueous solution, with an initial MO concentration of 50 mg·L^{-1} at 25°C for 90 min and the dye desorption step was performed with 50 mL of ethanol, using the same values for adsorbent mass (m = 0.2 g) and contact time.

3. Results and discussion

3.1. Characterization of activated carbon samples

3.1.1. Yield of activated carbon

The yield of activated carbon produced under various conditions is shown in Table 2. The mass of the samples was recorded before and after activation, with the final mass being determined as soon as the sample was removed from the furnace. Because *Brachychiton populneus* is a lignocellulosic material, the yield of activated carbon decreases with increasing activation time. During activation or carbonization, these polymeric structures decompose and liberate most of the non-carbon elements, primarily hydrogen, oxygen, and nitrogen, in the form of liquids (called tars) and gases, leaving behind a rigid carbon skeleton in the form of aromatic sheets and strips. This finding is comparable to the one reported by [9,11,24] for the chemically produced activated carbon. As a result, the percent yield of activated carbon derived from biomass waste is projected to be lower than that acquired from non-renewable sources. However, in the industrial world, the low cost of raw materials has a greater impact than the yield % obtained [25].

3.1.2. Textural properties of the prepared activated carbon

The adsorption isotherm's shape can provide qualitative information about the adsorption process and the amount of available surface area for the adsorbate. The nitrogen adsorption/desorption isotherms for ACs are shown in Fig. 2. According to the IUPAC classification, all isotherms of all carbon display a combination of Type I and Type IV isotherms, which are typical of microporous materials with the presence of mesopores [14,26]. Type IV isotherms with a type H4 hysteresis loop associated with monolayer–multilayer

adsorption followed by capillary condensation in small slit-like holes exist at intermediate and high relative pressures [27]. The abrupt step-down of the desorption branch is a distinguishing feature of the H4 loop. This is usually found in a narrow range of P/P_0 ~ 0.4–0.5 for nitrogen, at temperatures of 77K.

Table 3 shows the textural analysis results for all of the adsorbents investigated. These materials are mesoporous (2 nm < d < 50 nm) based on pore size measurements. Furthermore, for carbons activated by NaOH, the volume of the mesopores is greater than that of the micropores, indicating a high mesoporosity, but for carbons activated by $FeCl_3$, the volume of the micropores represents a high microporosity [24]. Because the reaction rate is faster at a higher activation temperature and a longer activation time, the values of the activated carbon surface demonstrate the effect of increasing the temperature and activation time [9,27,28].

The surface morphology of ACs (CAB4 and CAF8) was studied using SEM. The generated ACs have a significant amount of porosity, as can be seen in the SEM images (Fig. 3). The structure is asymmetrical, and the existence of pores is strongly defined, as predicted by the N_2 adsorption isotherms data (Table 3). The amplification utilized in SEM, on the other hand, largely revealed the ACs macroporosity (>50 nm), while microporosity was not found.

According to all of these results, the textural features of these adsorbents are highly reliant on the temperature and calcination time, as well as the mode of chemical activation. As a consequence, all of these materials have large specific surfaces that are suitable to organic pollutant adsorption in the aqueous phase.

3.1.3. Chemical surface characterization

The infrared spectra of the activated carbons show that the surface functional groups of the activated carbons do not exhibit significant differences, independently of the activating agent used. For this reason, only two spectra are shown in Fig. 4. A wide band between 3,400 and 3,200 cm^{-1} could be assigned to O–H stretching. This band indicates the presence of carboxyl groups, phenols or alcohols. The band observed at about 2,900 and 2,850 cm^{-1} corresponds to aliphatic C–H stretching. Aromatic C=C ring stretching was observed at 1,600–1,550 cm^{-1}. Aromatic C=C peaks are an

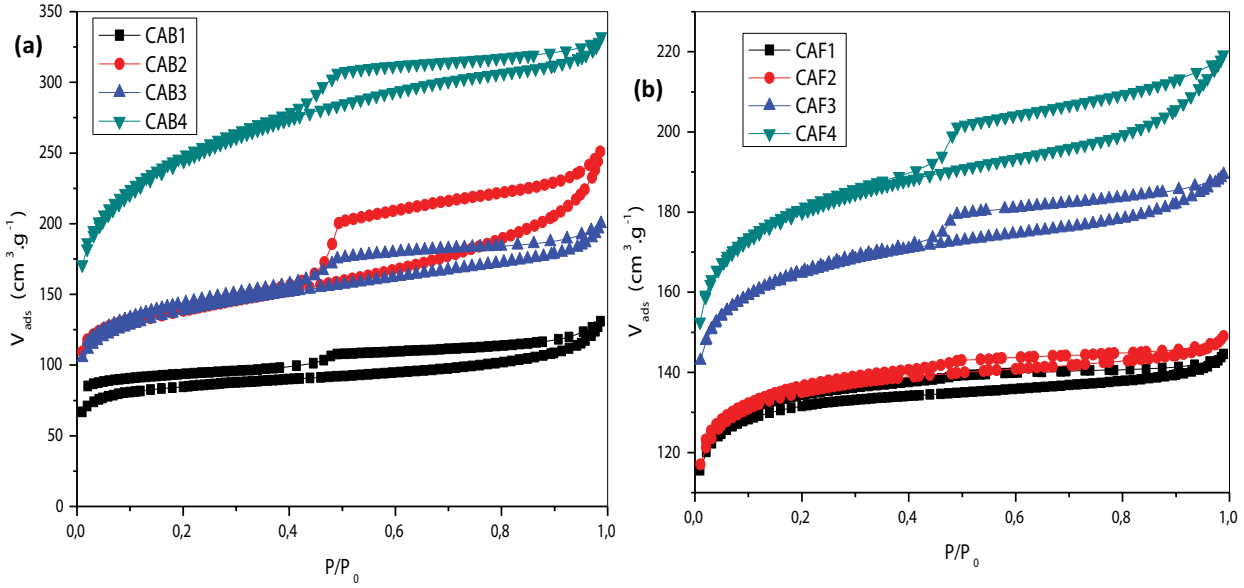

Fig. 2. Adsorption/desorption isotherms of N_2 (a) activated with NaOH and (b) activated with $FeCl_3$.

Table 3
Texturales properties of the produced carbons

Activated carbon	S_{BET} ($m^2 \cdot g^{-1}$)	S_{micro} ($m^2 \cdot g^{-1}$)	S_{ext} ($m^2 \cdot g^{-1}$)	V_{micro} ($cm^3 \cdot g^{-1}$)	V_{mes} ($cm^3 \cdot g^{-1}$)	V_{tot} ($cm^3 \cdot g^{-1}$)	d_m (nm)
CAB1	266.05	183.59	82.47	0.095	0.097	0.191	2.879
CAB2	443.45	250.55	192.90	0.129	0.238	0.368	3.319
CAB3	444.77	234.46	210.31	0.121	0.178	0.298	2.684
CAB4	803.38	316.86	486.53	0.163	0.340	0.503	2.505
CAF1	402.17	339.65	62.52	0.176	0.045	0.221	2.200
CAF2	415.32	335.03	80.29	0.173	0.055	0.228	2.198
CAF3	508.86	396.09	112.77	0.205	0.086	0.291	2.285
CAF4	557.96	416.36	141.60	0.216	0.120	0.335	2.404

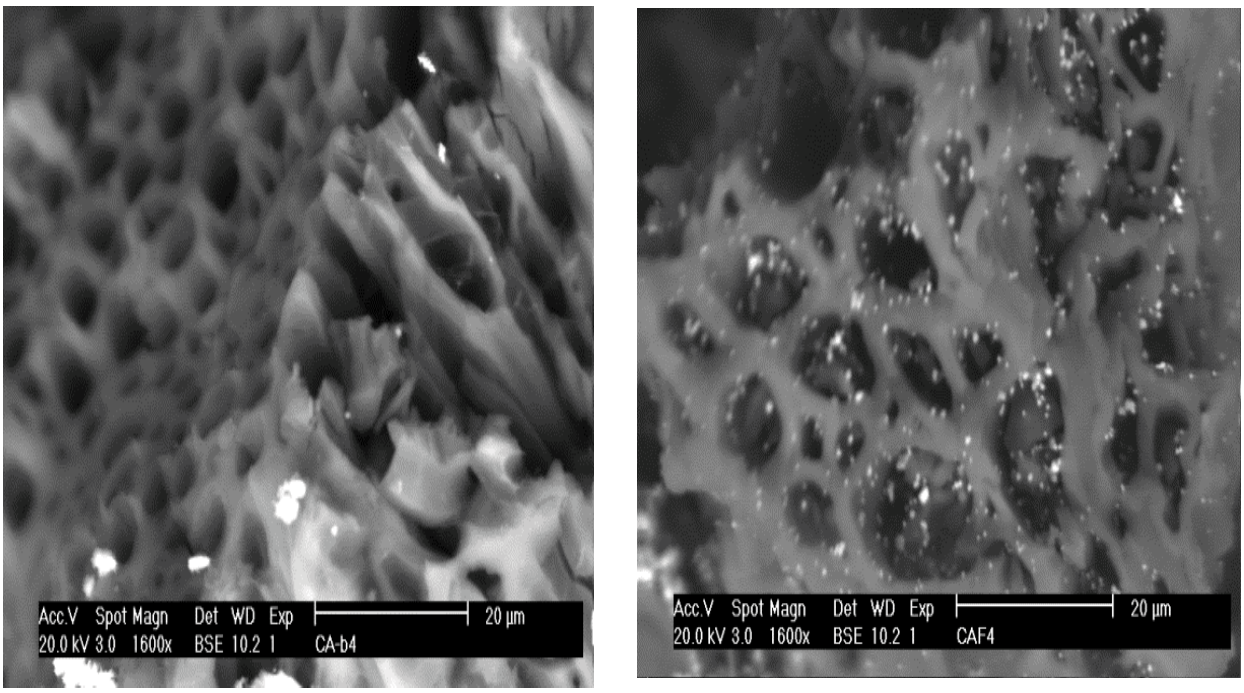

Fig. 3. SEM image of the activated carbon (CAB4 and CAF4).

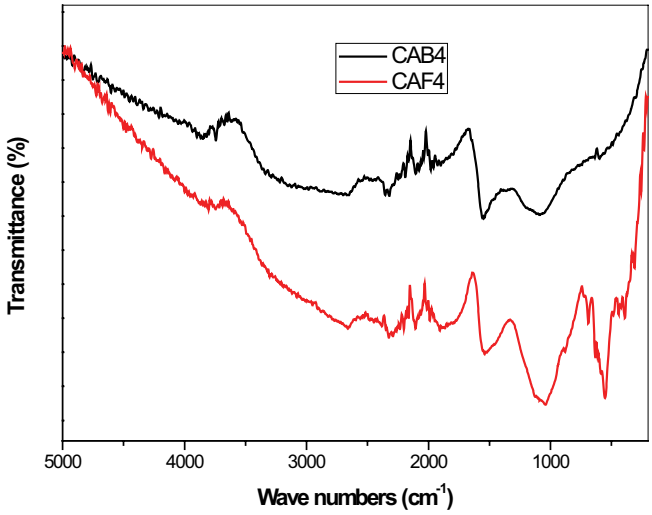

Fig. 4. FTIR spectra of prepared activated carbon (CAB4 and CAF4).

indication of benzene-like rings. The band at 1,000–1,200 cm^{-1} are assigned to C–O stretching in acids, alcohols, phenols and esters. The band at 812–400 cm^{-1} could be assigned to angular deformation out-of-plane of C–H bond of substituted aromatic rings [27,29].

The Boehm titration results (Table 4) show a weak acidity of less than 0.9 mmol·g^{-1} and a relatively strong basicity of more than 1 mmol·g^{-1} for all the materials activated by NaOH, there insues that the majority of the functional groups of the surface adsorbents are basic. This result is in agreement with the values of pH_{pzc} higher than 8. However, for all the materials activated by $FeCl_3$, the concentrations of the acid and basic sites are much lower than 1 mmol·g^{-1}, which confirms the almost neutral pH_{pzc} values.

3.2. Statistical analysis of the regression equation

Table 5 shows the main effects of variables (b_i) and their interaction effects (b_{ij}), as well as the model coefficients and standard coefficient regression values determined with Minitab 18. The best fitted models included temperature, time, activation agent and the interaction terms was determined for yield, total pore volume and percent removal of methyl orange. The equations for modeling are as follows:

$$Y_1 = 57.956 + 1.869x_1 + 7.549x_2 + 4.026x_3 + 1.131x_1x_2 + 0.189x_1x_3 - 0.226x_2x_3 - 2.439x_1x_2x_3 \quad (4)$$

$$Y_2 = 0.304 - 0.035x_1 + 0.052x_2 + 0.054x_3 - 0.008x_1x_2 - 0.041x_1x_3 + 0.008x_2x_3 + 0.001x_1x_2x_3 \quad (5)$$

$$Y_3 = 59.29 - 4.167x_1 + 23.497x_2 + 7.415x_3 + 0.14x_1x_2 + 2.508x_1x_3 + 4.987x_2x_3 + 1.59x_1x_2x_3 \quad (6)$$

To establish the significance of the main factors and their interactions, the statistical approach of ANOVA was

Table 4
Chemical characteristics of the synthesized ACs

Activated carbon	Acid group (mmol·g^{-1})			Total acid group (mmol·g^{-1})	Total based group (mmol·g^{-1})	pH_{pzc}
	Carboxylic	Lactonic	Hydroxylic			
CAB1	0.51	0.10	0.22	0.83	1.06	8.05
CAB2	0.57	0.11	0.19	0.87	1.25	8.17
CAB3	0.60	0.12	0.18	0.90	1.56	8.25
CAB4	0.67	0.08	0.16	0.91	1.82	8.42
CAF1	0.17	0.03	0.23	0.43	0.13	6.61
CAF2	0.26	0.12	0.10	0.48	0.17	6.55
CAF3	0.38	0.03	0.30	0.71	0.24	6.69
CAF4	0.41	0.04	0.34	0.79	0.30	6.80

Table 5
Statistical parameters for 2^3 designs

Responses	Yield (Y_1)		Total volume of the pores (Y_2)		Percent removal of methyl orange (Y_3)	
Term	Effect	Coef.	Effect	Coef.	Effect	Coef.
Constant		57.956		0.304		59.290
x_1	3.737	1.869	–0.071	–0.035	–8.335	–4.167
x_2	15.187	7.594	0.104	0.052	46.995	23.497
x_3	8.052	4.026	0.108	0.054	14.830	7.415
x_1x_2	2.263	1.131	–0.016	–0.008	0.280	0.140
x_1x_3	0.378	0.189	–0.082	–0.041	5.015	2.508
x_2x_3	–0.453	–0.226	0.016	0.008	9.955	4.978
$x_1x_2x_3$	–4.877	–2.439	0.002	0.001	3.180	1.590
	R-Sq = 99.96%		R-Sq = 99.98%		R-Sq = 99.98%	
	R-Sq(Adj) = 99.71%		R-Sq(Adj) = 99.89%		R-Sq(Adj) = 99.81%	

applied. Table 6 shows the ANOVA results for main effects, 2-way interactions, and 3-way interactions. The sum of the squares used to estimate factors effect; Fisher's *F*-ratios and *P*-values were also represented. The preciousness of a factor in the model estimated by its sum of squares (SS). In such a way that significance of the factor in the process increases when SS value rises.

Each factor's main effects and interaction effects with a *P*-value less than 0.05 are considered potentially significant, while values more than 0.1 suggest that the model term is not significant. As some of the coefficients in Eqs. (4)–(6) are insignificant, the final empirical models for yield, total pore volume, and methyl orange removal percent become:

$$Y_1 = 57.956 + 1.869x_1 + 7.594x_2 + 4.026x_3 - 2.439x_1x_2x_3 \quad (7)$$

$$Y_2 = 0.304 - 0.035x_1 + 0.052x_2 + 0.054x_3 - 0.008x_1x_2 - 0.041x_1x_3 + 0.008x_2x_3 + 0.001x_1x_2x_3 \quad (8)$$

$$Y_3 = 59.29 - 4.167x_1 + 23.497x_2 + 7.415x_3 + 2.508x_1x_3 + 4.978x_2x_3 + 1.59x_1x_2x_3 \quad (9)$$

To test the model's reliability, an analysis of variance (ANOVA) was used. The predicted and experimental findings are in good agreement, as shown in Fig. 5. The model's adequacy and quality were assessed using the correlation coefficient R^2, which was determined to be 0.99, meaning that the model can explain 99% of the dye removal.

3.3. Analysis the effects of factorial design experiments

The main effect plot of the studied factors represents the deviations of the average between the high and low level for each factor. When the effect of a factor is positive, the response (*Y*) increases as the factor changes from its low to its high levels, and vice versa. An interaction between two factors is in effect when the change in the surface area from the low to high levels of a factor is dependent on the level of a second factor, that is, when the lines do not run parallel [30].

3.3.1. Main and interaction effects on the yield of activated carbon (Y_1)

According to the results on Table 6 and graphics of Fig. 6b, the temperature of calcination (b_2 = 7.594) and the activation time (b_3 = 4.026) appear as the most influent parameters on the yield of activated carbon, as witnessed

Table 6
Analysis of variance (ANOVA) for responses

Responses	Source	DF	Seq. SS	Adj. SS	Adj. MS	*F*-value	*P*-value
Yield (Y_1)	Main effects	3	618.944	618.944	206.315	503.810	0.027
	x_1	1	27.938	27.938	27.938	68.220	0.064
	x_2	1	461.320	461.320	461.320	1126.510	0.016
	x_3	1	129.686	129.686	129.686	316.680	0.030
	2-way interactions	2	10.647	10.647	5.324	12.850	0.161
	x_1x_2	1	10.238	10.238	10.238	25.000	0.105
	x_2x_3	1	0.410	0.410	0.410	0.700	0.443
	3-way interactions	1	47.580	47.580	47.580	116.190	0.049
	$x_1x_2x_3$	1	47.580	47.580	47.580	116.190	0.049
	Residual error	1	0.285	0.285	0.285		
	Total	7	677.456				
	S = 0.5339 R-Sq = 99.96% R-Sq(Adj) = 99.71%						
Total volume of the pores (Y_2)	Main effects	3	0.05556	0.05556	0.01852	1641.77	0.018
	x_1	1	0.01020	0.01020	0.01020	904.430	0.021
	x_2	1	0.02191	0.02191	0.02191	1942.49	0.014
	x_3	1	0.02344	0.02344	0.02344	2078.40	0.014
	2-way interactions	3	0.01464	0.01464	0.00488	432.790	0.035
	x_1x_2	1	0.00053	0.00053	0.00053	47.5400	0.092
	x_1x_3	1	0.01357	0.01357	0.01357	1202.99	0.018
	x_2x_3	1	0.00054	0.00054	0.00054	47.8300	0.0191
	Residual Error	1	0.00001	0.00001	0.00001		
	Total	7	0.07022				
	S = 0.00335 R-Sq = 99.98% R-Sq(Adj) = 99.89%						
Percent removal of methyl orange (Y_3)	Main effects	3	4,995.960	4,995.960	1,665.290	10,620.460	0.007
	x_1	1	138.940	138.940	138.940	886.130	0.021
	x_2	1	4,417.060	4,417.060	4,417.060	28,170.030	0.004
	x_3	1	439.860	439.860	439.860	2,805.220	0.012
	2-way interactions	2	248.500	248.500	124.250	792.430	0.025
	x_1x_2	1	50.300	50.300	50.300	320.790	0.036
	x_2x_3	1	198.200	198.200	198.200	1,264.060	0.018
	3-way interactions	1	20.220	20.220	20.220	128.980	0.056
	$x_1x_2x_3$	1	20.220	20.220	20.220	128.980	0.056
	Residual error	1	0.160	0.160	0.160		
	Total	7	5,264.750				
	S = 0.3960 R-Sq = 98.98% R-Sq(Adj) = 99.81%						

Note: DF: degree of freedom, Seq. SS: sequential sum of squares, Adj. SS: adjusted sum of squares, Adj. MS: adjusted mean sum of squares, *F*: Fischer's variance ratio (factor *F*) and *p*: probability.

by a shorp slop with a negative influence. In contrast, the activation agent (x_1) has a minor impact on the yield of active carbon. Nevertheless, the interaction effects seem to be insignificant in Fig. 6b. Wherefore, it is essential to use a low temperature of activating agent so as to obtain a higher yield in active carbon.

According to several researchers in the literature [24], the AC yield decreases as the activation temperature, activation period, and chemical impregnation ratio increase. The elimination of volatiles and contaminants from the sample due to thermal decomposition and carbon monoxide emission via the C–CO_2 reaction increased as the activation temperature rised, resulting in a drop in sample weight [31].

3.3.2. Main and interaction effects on the total volume of the pores (Y_2)

The total volume of the pores of activated carbon obtained from biomass varies between 0.191 and 0.503 $cm^3 \cdot g^{-1}$, as indicated in Table 3. Fig. 7a illustrates the main effects of each parameter on the total volume of the pores. The effects of temperature and time factors are positive, that is, as the factor goes from low to high, the total volume of the pores increases. When temperature and time factors are at their highest, the mean BET is higher than when they are at their lowest. The opposite is true for the agent activation factor. Furthermore, as evidenced by the longer vertical line [30],

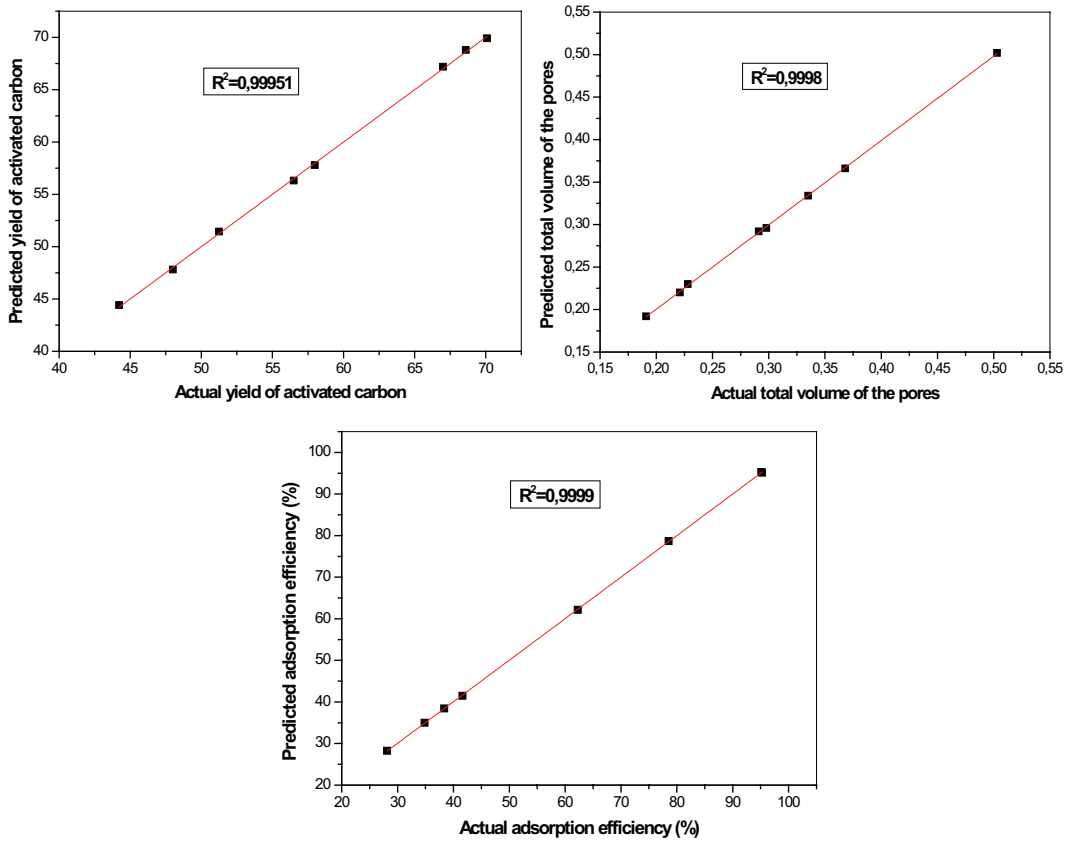

Fig. 5. Comparison plot between the predicted and corresponding experimental results.

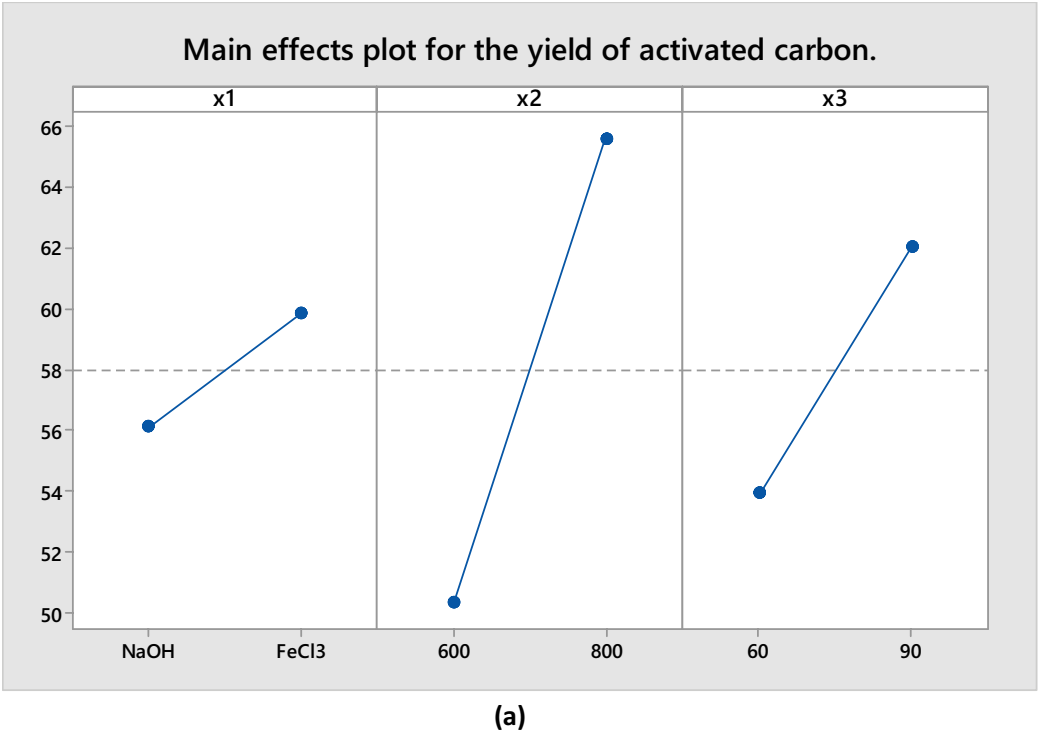

(a)

(Continued)

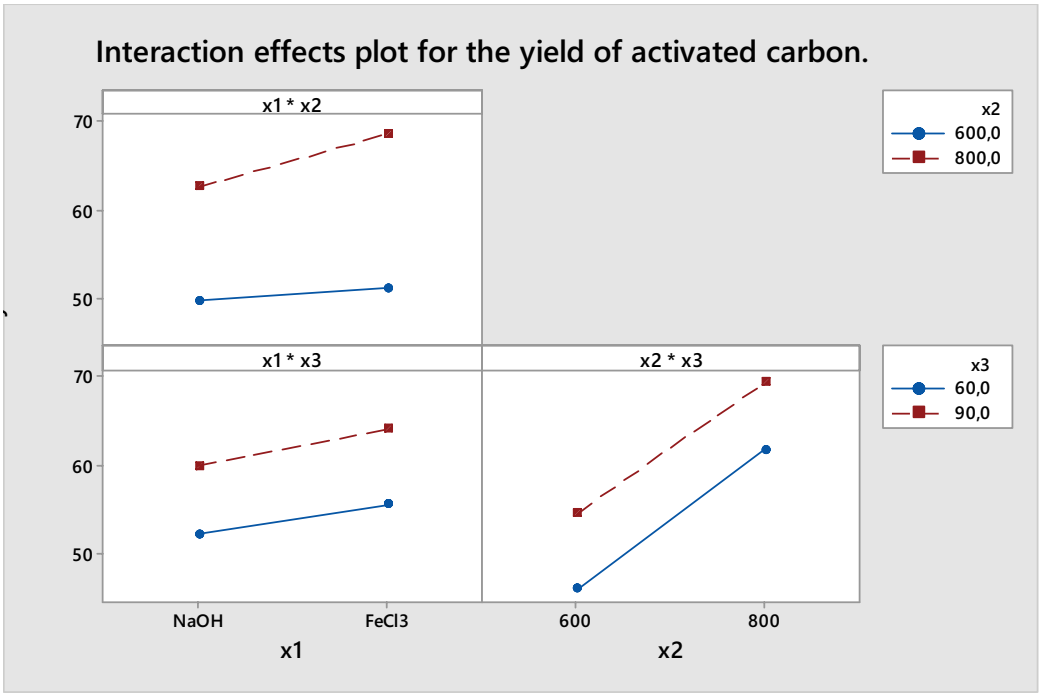

(b)

Fig. 6. Main effects plot (a) and interaction effects plot (b) for yield.

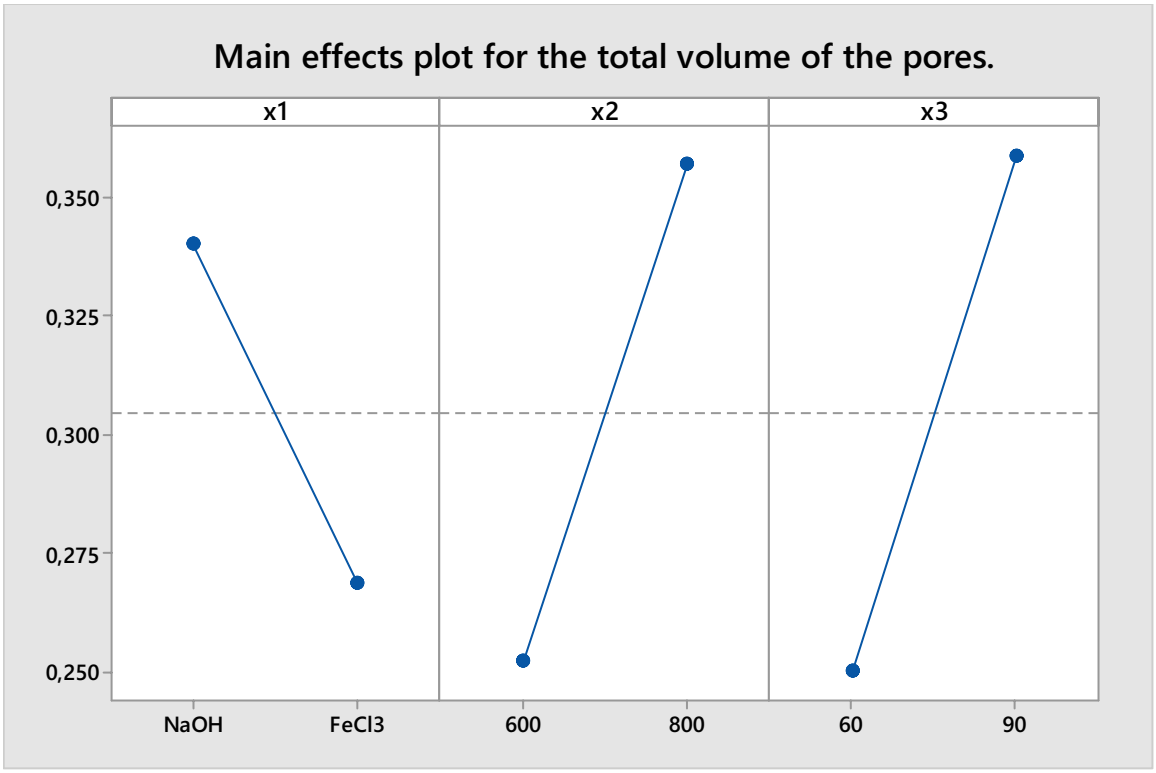

(a)

(Continued)

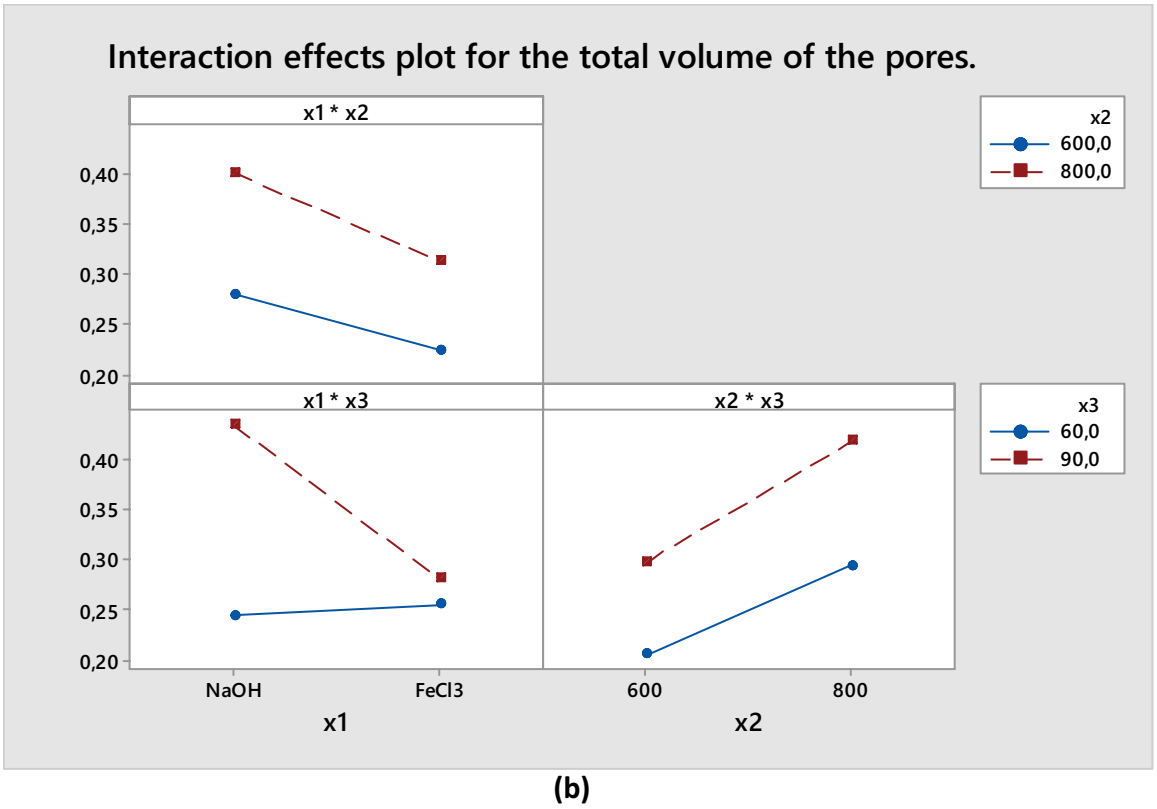

Fig. 7. Main effects plot (a) and interaction effects plot (b) for total volume of the pores.

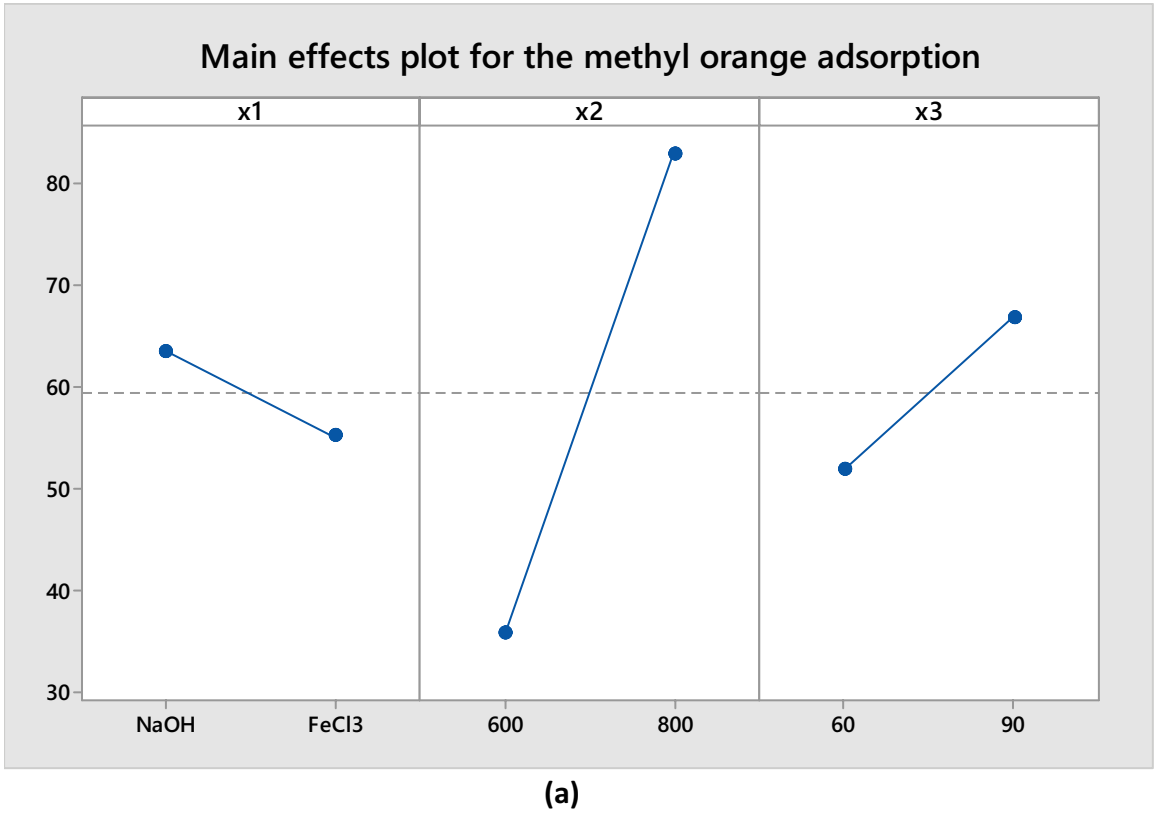

(Continued)

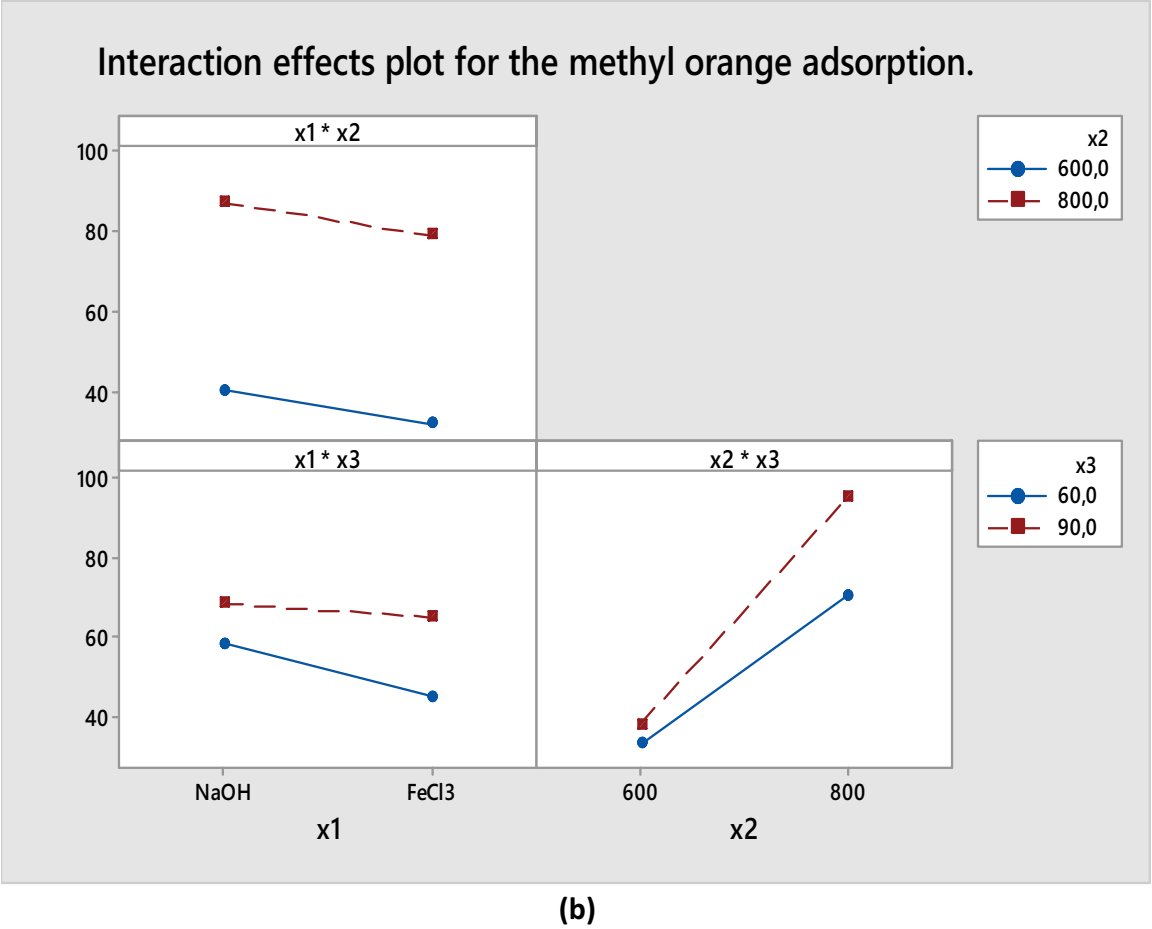

Fig. 8. Main effects plot (a) and interaction effects plot (b) for MO removal.

temperature had a bigger effect on overall volume of the pores.

Fig. 7b shows that the interaction agent activation and time (b_{13}) was stronger than between temperature and time (b_{23}) and between temperature and agent activation (b_{12}).

3.3.3. Main and interaction effects on the percent removal of methyl orange (Y_3)

After examining the main effects of each parameter on the dye adsorption graphs in Fig. 8a and the coefficients of Eq. (6), it was determined that the calcination temperature was the most critical variable of the whole adsorption technique (b_2 = 23.497). When this coefficient was positive, it signified that MO removal was favored at high temperatures [32].

The interaction effects of the factors activation temperature, activation time, and activation chemical agent on MO elimination are shown in Fig. 8b. These results show a weak interaction (b_{23}) between increasing the activation temperature and activation duration and the removal of MO on AC.

3.4. Adsorbent recycling

Fig. 9 displays the percentage removal of dyes after each regeneration period. It was found that, in the first cycles,

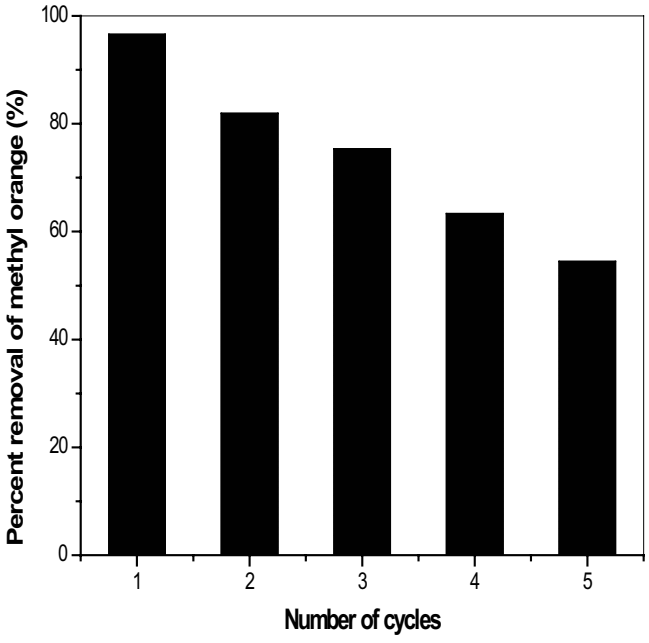

Fig. 9. Reusability cycles of prepared activated carbon CAB4.

the percentage elimination was between 100%–75% and then approached 55% in the five cycle. The reusability test reported that the CAB4 is easily regenerated and has the potential to be reused in many cycles of treatment.

4. Conclusion

Brachychiton populneus was used as precursor to prepare mesoporous-activated carbon with high surface area, sufficient yield of carbon, and high dye removal. A complete factorial design was conducted to study the effects of three activated carbon preparation variables, which were the activation temperature, activation time, and activation chemical agent on the activated carbon yield, total volume of the pores and the removal of methyl orange. The characterization of activated carbons and statistical analysis of factorial design experiments, the yield was found to decrease with increasing activation temperature and activation time. It was found that the removal of methyl orange increases with the increasing of activation temperature and the interaction between agent chemical, temperature and time of calcination. The optimum conditions to prepare activated carbons from *Brachychiton populneus* by chemical activation were obtained using 800°C activation temperature, 90min activation time, and NaOH activating agent. The present study concludes that the *Brachychiton populneus* could be employed as low-cost adsorbent as alternative to commercial activated carbon for the removal of dyes from water and waste water.

Acknowledgments

This work was supported by the Ministère de l'Enseignement Superieur et de la Recherche Scientifique of Algeria under Research Project PRFU_No. A16N01UN180120190001.

References

[1] N.M. Nor, L.C. Lau, K.T. Lee, A.R. Mohamed, Synthesis of activated carbon from lignocellulosic biomass and its applications in air pollution control—a review, J. Environ. Chem. Eng., 1 (2013) 658–666.
[2] F. Gao, Y.-h. Zang, Y. Wang, C.-q. Guan, J.-y. Qu, M.-b. Wu. A review of the synthesis of carbon materials for energy storage from biomass and coal/heavy oil waste, New Carbon Mater., 36 (2021) 34–48.
[3] S.Z. Naji, C.T. Tye, A review of the synthesis of activated carbon for biodiesel production: precursor, preparation, and modification, Energy Convers. Manage.: X, 13 (2022) 100152, doi: 10.1016/j.ecmx.2021.100152.
[4] H. Tounsadi, A. Khalidi, M. Farnane, M. Abdennouri, N. Barka, Experimental design for the optimization of preparation conditions of highly efficient activated carbon from *Glebionis coronaria* L. and heavy metals removal ability, Process Saf. Environ. Prot., 100 (2016) 710–723.
[5] D. Savova, E. Apak, E. Ekinci, F. Yardim, N. Petrov, T. Budinova, M. Razvigorova, V. Minkova, Biomass conversion to carbon adsorbents and gas, Biomass Bioenergy, 21 (2001) 133–142.
[6] S. Mateo, A.J. Moya, G. Hodaifa, S. Sánchez, M. Cuevas, Valorization of olive endocarp from olive oil and table olive processing as a low-cost bioadsorbent for the removal of furfural from aqueous solutions, J. Water Process Eng., 44 (2021) 102442, doi: 10.1016/j.jwpe.2021.102442.
[7] Z. Belala, M. Belhachemi, M. Jeguirim, Activated carbon prepared from date pits for the retention of NO_2 at low temperature, Int. J. Chem. Reactor Eng., 12 (2014) 717–726.
[8] K. Rida, A. Bouanika, M. Boudellal, A. Boukhemkhem, Valorization of a natural residue (sawdust) as adsorbent to remove the acetic acid in aqueous solutions, Desal. Water Treat., 56 (2015) 2731–2738.
[9] S. Benhabiles, K. Rida, Production of efficient activated carbon from sawdust for the removal of dyes in single and binary systems – a full factorial design, Part. Sci. Technol.: An Int. J., 39 (2021) 237–251.
[10] E. Rosson, P. Sgarbossa, M. Mozzon, F. Venturino, S. Bogialli, A. Glisenti, A. Talon, E. Moretti, S.M. Carturan, S. Tamburini, A. Famengo, A.P. da Costa Ribeiro, S. Benhabiles, R. Kamel, F. Zorzi, R. Bertani, Novel correlations between spectroscopic and morphological properties of activated carbons from waste coffee grounds, Processes, 9 (2021) 1637, doi: 10.3390/pr9091637.
[11] F. Wang, Y.-q. Dang, X. Tian, S. Harrington, Y.-q. Ma. Fabrication of magnetic activated carbons from corn cobs using the pickle liquor from the surface treatment of iron and steel, New Carbon Mater., 33 (2018) 303–309.
[12] Y. Yang, F.S. Cannon, Biomass activated carbon derived from pine sawdust with steam bursting pretreatment; perfluorooctanoic acid and methylene blue adsorption, Bioresour. Technol., 344 (2022) 126161, doi: 10.1016/j.biortech.2021.126161.
[13] A. Regti, M.R. Laamari, S.-E. Stiriba, M. El Haddad, Use of response factorial design for process optimization of basic dye adsorption onto activated carbon derived from Persea species, Microchem. J., 130 (2017) 129–136.
[14] T. Tay, S. Ucar, S. Karagöz, Preparation and characterization of activated carbon from waste biomass, J. Hazard. Mater., 165 (2009) 481–485.
[15] Y. Liu, P. Liu, L. Li, S. Wang, Z. Pan, C. Song, T. Wang, Fabrication of biomass-derived activated carbon with interconnected hierarchical architecture via H_3PO_4-assisted KOH activation for high-performance symmetrical supercapacitors, Electroanal. Chem., 903 (2021) 115828, doi: 10.1016/j.jelechem.2021.115828.
[16] J. Bedia, M. Peñas-Garzón, A. Gómez-Avilés, J.J. Rodriguez, C. Belver, Review on activated carbons by chemical activation with $FeCl_3$, Carbon Res., 6 (2020) 21–46.
[17] M. Danish, T. Ahmad, A review on utilization of wood biomass as a sustainable precursor for activated carbon production and application, Renewable Sustainable Energy Rev., 87 (2018) 1–21.
[18] J. Jjagwe, P. Wilberforce Olupot, E. Menya, H. Mpagi Kalibbala, Synthesis and application of granular activated carbon from biomass waste materials for water treatment: a review, J. Bioresour. Bioprod., 6 (2021) 292–322.
[19] B.G.H. Briton, B.K. Yao, Y. Richardson, L. Duclaux, L. Reinert, Y. Soneda, Optimization by using response surface methodology of the preparation from plantain spike of a micro-/mesoporous activated carbon designed for removal of dyes in aqueous solution, Arabian J. Sci. Eng., 45 (2020) 7231–7245.
[20] Y. El Maguana, N. Elhadiri, M. Bouchdoug, M. Benchanaa, Study of the influence of some factors on the preparation of activated carbon from walnut cake using the fractional factorial design, J. Environ. Chem. Eng., 6 (2018) 1093–1099.
[21] G. Jaria, C.P. Silva, J.A.B.P. Oliveira, S.M. Santos, M.V. Gil, M. Otero, V. Calisto, V.I. Esteves, Production of highly efficient activated carbons from industrial wastes for the removal of pharmaceuticals from water—a full factorial design, J. Hazard. Mater., 370 (2019) 212–218.
[22] K. Patidar, M. Vashishtha, Optimization of process variables to prepare mesoporous activated carbon from mustard straw for dye adsorption using response surface methodology, Water Air Soil Pollut., 231 (2020) 526–543.
[23] K. Ennaciri, A. Baçaoui, M. Sergent, A. Yaacoubi, Application of fractional factorial and Doehlert designs for optimizing the preparation of activated carbons from Argan shells, Chemom. Intell. Lab. Syst., 139 (2014) 48–57.
[24] P.P.M. Fung, W.H. Cheung, G. McKay, Systematic analysis of carbon dioxide activation of waste tire by factorial design, Chin. J. Chem. Eng., 20 (2012) 497–504.
[25] S.M. Yakout, G. Sharaf El-Deen, Characterization of activated carbon prepared by phosphoric acid activation of olive stones, Arabian J. Chem., 9 (2016) S1155–S1162.

[26] N. Isoda, R. Rodrigues, A. Silva, M. Gonçalves, D. Mandelli, F.C.A. Figueiredo, W.A. Carvalho, Optimization of preparation conditions of activated carbon from agriculture waste utilizing factorial design, Powder Technol., 256 (2014) 175–181.
[27] A. Kumar, H.M. Jena, Preparation and characterization of high surface area activated carbon from Fox nut (*Euryale ferox*) shell by chemical activation with H_3PO_4, Results Phys., 6 (2016) 651–658.
[28] U.T. Un, F. Ates, N. Erginel, O. Ozcan, E. Oduncu, Adsorption of Disperse Orange 30 dye onto activated carbon derived from Holm Oak (*Quercus Ilex*) acorns: a 3^k factorial design and analysis, J. Environ. Manage., 155 (2015) 89–96.
[29] B.G.H. Briton, B.K. Yao, Y. Richardson, L. Duclaux, L. Reinert, Y. Soneda, Optimization by using response surface methodology of the preparation from plantain spike of a micro-/mesoporous activated carbon designed for removal of dyes in aqueous solution, Arabian J. Sci. Eng., 45 (2020) 7231–7245.
[30] D. Bingol, N. Tekin, M. Alkan, Brilliant Yellow dye adsorption onto sepiolite using a full factorial design, Appl. Clay Sci., 50 (2010) 315–321.
[31] I.A.W. Tan, A.L. Ahmad, B.H. Hameed, Optimization of preparation conditions for activated carbons from coconut husk using response surface methodology, Chem. Eng. J., 137 (2008) 462–470.
[32] S. Saadat, A. Karimi-Jashni, Optimization of Pb(II) adsorption onto modified walnut shells using factorial design and simplex methodologies, Chem. Eng. J., 173 (2011) 743–749.